Design and Performance Analysis of MIMO Patch Antenna using Superstrate for Minimization of Mutual Coupling

[1]PALLAVI H. V., [2]A. P. JAGADEESH CHANDRA, [3]PARAMESHA
[1]Department of Electronics and Communication Engineering, Government Engineering College, Hassan, Karnataka, 573202, INDIA
[2]Department of Electronics and Communication Engineering, Adichunchanagiri Institute of Technology, Chikkamagaluru, Karnataka, INDIA
[3]Department of Electronics and Communication Engineering, Central University of Karnataka, Kalburgi, INDIA

Abstract: - Antennas play a critical role in wireless communications. Where the existing design focuses only on frequency reconfiguration, but it does not take advantage of the entire frequency and power spectrum. Therefore, the honeycomb-shaped Metamaterial cells used in the suggested antenna design serve as a superstrate for microstrip patch antennas with an extensive range of actual negative permittivity and permeability, as well as a refractive index feature. Also, to reduce mutual coupling in current printed and other antennas. The superstrate microstrip antenna which is based on metamaterial through RF MEMS Varactor diode switching is proposed in this paper. Based on a microstrip antenna, metamaterials in the shape of circular and hexagonal arrays are employed as the superstrate. Also, the superstrate layers serve as a random, providing strength to the entire structure while also improving other antenna metrics such as gain and bandwidth. The design outputs for several metamaterial superstrates in terms of gain, reflection coefficient (S11), and bandwidth are evaluated based developed model and compared with existing works after the addition of varactor diode switches to the proposed superstrate, which also allows for frequency reconfiguration. As a result, the suggested antenna was designed to reduce mutual coupling and improve system performance in 5G technology, specifically in mm-wave applications. The obtained results for metamaterial superstrate designs demonstrate high bandwidth and gain behaviour.

Key-Words: - Metamaterial, Superstrate, Patch, Gain, Bandwidth, Frequency, Mutual coupling

Received: July 9, 2021. Revised: May 13, 2022. Accepted: June 8, 2022. Published: July 4, 2022.

1 Introduction

With the rapid advancement of 5G technologies used in wireless communication systems and has huge demand in terms of performance levels in terms of high throughput and low latency for mobile communications apps and primarily consist of extremely high data rates. 5G is a next-generation telecommunications technology that will enable the rate at which the packet transmits in the range of 10Mbps to 10Bbps [1, 2]. Microwave refers to ultra-high frequency (UHF) frequencies ranging from 300 MHz to 3000 MHz as well as extremely high frequency (EHF) frequencies ranging between 30 GHz to 300 GHz. In general, both licensed authorized and unauthorized microwave bands are frequently operating in both bands such as super-high frequency (SHF) and extra-high frequency (EHF) bands, with frequencies ranging from 3 GHz to 30 GHz. The signal will typically travel at a low frequency. As a result, lower frequency throughput suffers, and vice versa. Another current advantage of the network's high density is that it will change the old network layout from cells that are formed as groups of more cells and covering more distances to more number of cells that are small that provide increased bandwidth and channel capacity while reducing power transmitted as they change to millimeter waves. The mm-Wave is an important feature of 5G systems and its role in systems that are related to cellular services for users [3][4]. [5] [6] propose mm-Wave for 5G cellular communication, whereas [7] [8] provide propagation models for 5G mm-Wave communication. Although the EHF range in the electromagnetic spectrum is suffering underutilized for wireless systems, still some communication systems are in the investigation for point to point, short-range and point to multipoint communication systems. High bandwidth and data rates, yet due to signal blockage and attenuation, these high frequencies will place limits on this

system. Thus, certain antennas, such as MIMO antennas, have been necessary for communication standards because they allow broadcast signal characteristics to be adjusted to match millimeter-wave[9]. 5G is a cutting-edge wireless system that was widely used in or before the 2020 years. The MIMO antenna system, which can give 9-99 times more than 4G and LTE systems in terms of bandwidth [10], is a critical component of 5G technology. High-speed data transmission that is combined through spectrum management via many antennas on a single physical substrate is a relatively latest demand in the recent wireless system. MIMO technology achieves this purpose by utilizing diversity gain to improve link reliability, data throughput, capacity, and range that are not possible achievable in a single-antenna system [11]. In terms of channel capacity, MIMO technology outperforms SIMO or MISO, but it has some drawbacks in terms of antenna correlation and space efficiency [12]. One of the most promising 5G technologies is multi-input and multi-output (MIMO). MIMO technology, which has been extensively investigated, can improve data transmission speed and give resistance to multiple paths fading. In a MIMO system, the transmitter or receiver must have two or more antenna elements [13]. The planned MIMO antenna, like certain designs [15], must inevitably produce adequate features for the future, and one of the critical variables is gain. However, because of design size constraints, numerous elements are positioned close together, generating mutual coupling and lowering the MIMO antenna's diversity performance [16]. Different decoupling procedures are studied and reported in the latest survey to minimize any effect of reciprocal coupling. Some parameters like parasitic which are etched, rings which are split resonators, bandgap electromagnetic strut, ure, and defective structures can all be employed to lessen mutual coupling in 5G antenna are designed using MIMO technology. To minimize mutual coupling, metamaterials are utilized and discussed in [17].

In MIMO antennas, the main effect coupling is mutual which is discussed in [18, 19, 20].Decoupling methods include defected ground structure (DGS) [21], parasitic element [22], electromagnetic band-gap (EBG) [23]-[25], neutralization line [26], asymmetric coplanar wall [27], optimization of topology [28], array-antenna decoupling surface (ADS) [29], decoupling ground [30], near-field resonator [31], polarization diversity [32], split ring resonator (SRR)All of the above-mentioned measures can successfully reduce mutual coupling. However, the vast majority of coupling has a limited coupling system that had a two-port antenna. To overcome the limitation of massive antenna coupling, a novel design must be developed.

The contribution of this paper,

- To reduce mutual coupling, Metamaterial Superstrate-based Micro Strip Patch Antenna is used.
- To limit wave propagation, circular or hexagonal shape metamaterial cells are designed.
- Adding varactor diode switches to the metamaterial superstrate for frequency reconfiguration.
- The MIMO antenna is provided to boost performance and provide strong isolation.

The rest of the work in this article is organized as below discussions: In 2nd subsection examines recent literature; Section 3 provides a detailed description of the suggested methodology; Section 4 reviews implementation outcomes; and Section 5 ends the article. Finally, all simulations were carried out using ANSYS HFSS.

2 Literature Survey

T. S. Rappaport, et al. [42] Recent advancements in millimeter-wave frequencies are being driven by increased demand for more throughput rate of data transmission over short distances multimedia users. Therefore, the best solution for enabling high-speed data in terms of Gbit/seconds in communications is deployment and discussed in [13] of wireless communications which will be operating at mm-wave frequencies. 8 Very broad bandwidths are available at those frequencies, and these bands are used in high throughput systems in wireless.

In [43] The antenna structure is physically modest because of the 60 GHz frequency and 5 mm free-space wavelength. High data rates can be achieved while avoiding co-channel interference thanks to the availability of 9 GHz bandwidth in the 60 GHz range. Although there are huge free-space losses at this frequency, big free-space losses 2 can be compensated for by using a high-gain antenna array. In the case of indoor radio communications, a human barrier can have a significant impact on the radio channel. To address this issue, high-gain antennas with beam directing capabilities are required.

Thummaluru, et.al [44] To achieve isolation greater than 15 dB, a mu negative meta-material was used in a band-stop filter and designed for two monopole antennas which used 0.16 edge separations, the limitation of these designs is the split concept used in ground plane and for matching, the series stub is

utilized and these are additional effects and not suitable in real-time applications. Jafargholi et al. [45] showed that a CLL-MTM superstrate is a suitable instrument for attenuating surface waves in antennae which are used in patch arrays the superstrates are based on CLCLL-MTM'she ability to build autonomously arrays its is based on the planar antenna is a key advantage. This method, however, is ineffective for larger patch array antennas. Jiang, et al [46] offers a new meta-surface superstrate for decoupling massive antenna arrays It should be emphasized that achieving high isolation of a two-port antenna is a rather simple process. However, establishing high isolation for larger arrays is a tough process due to mutual interactions between inner and outer array components making total decoupling difficult. Parchin, et. al [47] presented the smartphones that are based on 5G and 4G architectures which are designed using array-based multi-band slot antenna. The proposed design has a square ring that double-element slot radiators and is subjected to microstrip structures and allows for easy integration of RF and microwave circuits. Yang, et. Ojaroudi al [48] proposed FR4 based printed substrate of a thickness of 0.8mm which is connected by a coaxial wire, which can provide three-wide operational bandwidths for 5G technologies uses: 3288–3613 MHz and 1596–2837 MHz.

Desai et.al [49] a new dual branch multiband tiny slotted antenna tis are used in the broadcasting of digital devices, Wi-Fi, and sub-6 GHz 5G networks. At (750–790 MHz), the antenna possesses multiband characteristics. Patel, et al [50] square microstrip-based patch multiband antenna is proposed and it uses metamaterial and metamaterials have qualitatively new electromagnetic response functionalities are not exiting in present communication networks. The integration of antennae is easily present simultaneously at different frequencies. Chouhan, et al [51] Proposes a MIMO system that is based on a spider-shaped fractal that is used WLAN, WiMAX, Wi-Fi, C, and Bluetooth technologies. It consists of two fourth-generation microstrip line-fed antenna elements and two Y-shaped backplane structures linked to a shared half rectangular ground plane. Addepalli, et al [52] It is built with a hexagonal MIMO patch antenna. It comprises S-band (2-4 GHz), 2400-2480 MHz & 5150-5350 MHz used in WLAN, 3.1-10.6 GHz used in UWB, and X band used for 8-12 GHz. Gao, et al. [53] The antenna is composed of two modified coplanar waveguides (CPWs) that feed staircase-shaped radiating components for orthogonal radiation patterns, with a 45° rectangular stub between the CPWs to ensure excellent isolation. Kavitha, et al. [54] The Metamaterial Superstrate Antenna considerably contributes to the antenna's gain. The primary purpose of this research is to improve the gain and directivity of the Metamaterial Microstrip Patch Antenna used in Wireless Point-to-Point Communication applications like Dedicated Short-Range Communications (DSRC). Nazl, et al. [55] For 5G applications, a novel patch antenna for wideband antenna design in the sub-6 GHz range is being developed. The CST software was used to build and simulate the wideband antenna for the frequency band between 3.5 to 5 GHz. The antenna material is made up of Rogers RT5880 as a substrate with a thickness of 0.254 mm and a dielectric constant of 2.20, as well as copper material for the ground and patch of the antenna. Lee, et al. [56] In a MIMO-based antenna, the characters are separated into two radiating features and these are magnified using an SRR array structure. Where the designed antenna met under return loss of 10 dB condition in the Mobile-WiMAX frequency band. Two antenna elements are separated by 0.1mm. However, the antenna's performance has not been precisely assessed [42] The antenna [44] covers the 1.34–3.92 GHz and 4.34–6.34 GHz wideband frequency bands, and the two antenna elements are separated by 0.1mm. However, the antenna's performance has not been precisely assessed. [43] A human blockage on an indoor radio link could have a substantial influence on the radio channel. The research studies indicated a split in the ground plane as well as an additional series stub for matching, both of which are impractical [46]. It is difficult to obtain high isolation for larger arrays because mutual interactions between inner and outer array members make overall decoupling difficult [47], hence a novel method is required to deal with massive MIMO patch antenna arrays for 5G technology.

3 Metamaterial Superstrate based Micro Strip Patch Antenna

In superstrate, microstrip has a highgraded-index along with free space and it will reduce quality factor with sufficient dielectric resonator. The high dielectric material will reduce the size and slot significantly. MIMO patch antennas are frequently employed, making reciprocal coupling inevitable. Mutual coupling can generate excessive side lobes, gain decrease, and a huge voltage standing wave ratio (VSWR). A significant amount of scientific

effort has been spent on mutual coupling reductions over the previous few decades. But the existing work that has been suggested for the MIMO antenna arrays is not focused on the MIMO microstrip patch antenna system. To solve the aforementioned difficulties, a novel Metamaterial Superstrate-based Micro Strip Patch Antenna with reduced mutual coupling has been created to improve the antenna system's performance, as shown in figure 1.
The metamaterial cells employed in the suggested antenna design have the cell shape of a honeycomb and are used as a superstrate based on microstrip patch antennas with a wide range of effective negative permittivity and permeability, as well as a refractive index property, in the suggested framework. The frequency reconfiguration was accomplished by incorporating RF MEMS Varactor diode switches into the Metamaterial Superstrate. In addition, the MIMO antenna includes a 2 mm separation between antenna parts, which provides excellent isolation. As a result, the suggested antenna was developed to reduce mutual coupling and thereby improve system performance in 5G technology, particularly in mm-wave applications.

3.1 Estimation of the Design

A high-frequency structure simulator is used to analyze the performance of the suggested antenna structure (HFSS). The suggested structure is studied utilizing a variety of geometries, including microstrip patch antennas (MPAs), superstrate microstrip patch antennas (SMPAs), circles, and hexagonal array metamaterial. Consequently, the Roger RT Duroid 5880 Substrate and FR4 Metamaterial Superstrate with split ring resonator (SRR) were used in this research. The Metamaterial is utilized as a Superstrate, together with an array of patches, to boost the antenna gain and directivity. Also, a novel foraging and navigation optimization technique have been suggested to optimize antenna characteristics such as frequency, bandwidth, and beamwidth as shown in Fig1. The antenna parameters are selected optimally with the help of tuning the metamaterial superstrate permeability and permittivity values.
The steps that are involved in estimating a design.
Step 1: Set the resonant frequency $f_r = 30\ GHz$, and then calculate a single patch.
Step2: Maintain a $\frac{\lambda}{2}$ spacing between the patches and insert a honeycomb structure.
Step3: Measure the patch width with help eq (1)

$$W_P = \frac{C}{2f_r\sqrt{\frac{(\varepsilon_r+1)}{2}}} \quad (1)$$

where W_P is patch width,
c is representing the speed of the light i. e. , $c = 3 \times 10^8$
f_r be the resonant frequency
ε_r be the dielectric constant.

Step4: Calculate the length of the patch using eq. (2).

$$L_p = L_{peff} - 2\Delta L_p \quad (2)$$

Where is the actual length of the patch?
ΔL_p is the length of the patch generated as a result of the electrical distribution over the antenna?
Step 5: Derive ΔL_p by using the following equations.

$$L_{peff} = \frac{c}{2f_r\sqrt{\varepsilon_{reff}}} \quad (3)$$

$$\Delta L_p = 0.412h\frac{(\varepsilon_{reff}+0.3)\left(\frac{w_p}{h}+0.21\right)}{(\varepsilon_{reff-0.21})\left(\frac{w_p}{h}+0.80\right)} \quad (4)$$

where h be the substrate thickness
ε_{reff} be the effective dielectric constant.

Step 6: Derive h by applying the following equations.

$$\varepsilon_{reff} = \frac{\varepsilon_r+1}{2} + \frac{\varepsilon_r-1}{2}\left[1 + 12\frac{h}{w_p}\right]^{\frac{-1}{2}} \quad (5)$$

Step 7: Estimate the extent of the substrate.

$$L_g = 6h + L_p \quad (6)$$

Where is the length of the substrate?

Step 8: Calculate substrate width by applying the following equation.

$$W_g = 6h + W_p \quad (7)$$

Where denotes the width of the substrate. The ground plane's length and breadth are assumed to be the same as the substrate's length and width to improve performance.
Step 9: To calculate the length of the microstrip feed line, use the following equation.

$$L_f = \frac{1}{4}\lambda_g \quad (8)$$

where L_f is the microstrip feedline
λ_g be the guided wavelength
Step 10: Calculate and by executing the below equations.

$$\lambda_g = \frac{\lambda}{\sqrt{\varepsilon_{reff}}} \quad (9)$$

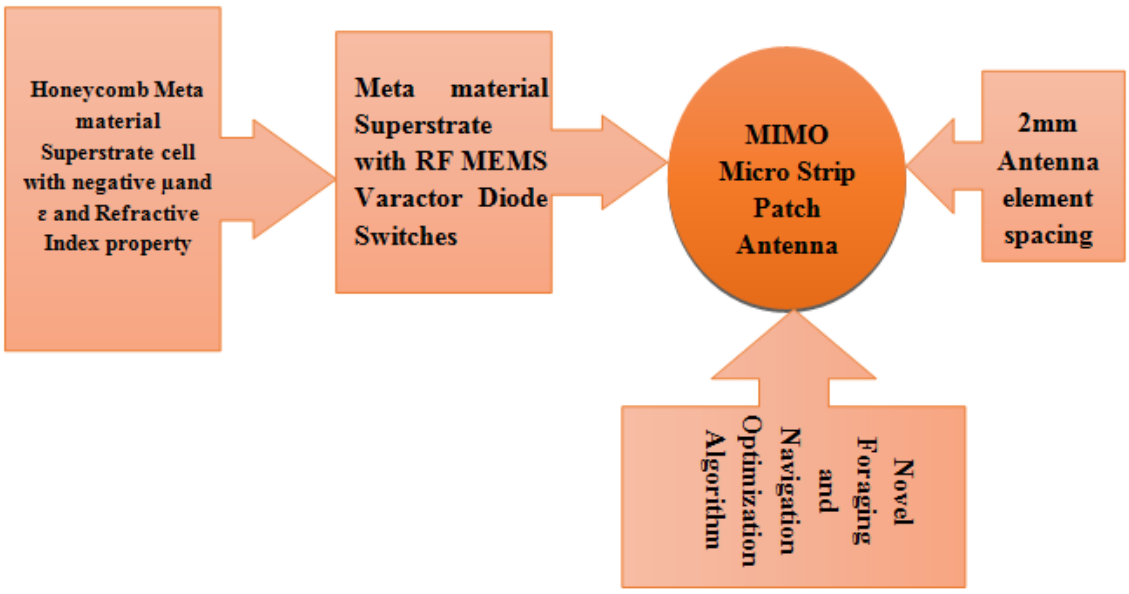

Fig. 1. Schematic representation of the suggested framework

Here,λ is signified as the wavelength, and it is considered using the equation provided below.

$$\lambda = \frac{c}{f_r} \quad (10)$$

Step 11: Apply the following calculation to get the feed line width.

$$W_f = \frac{7.48 \times h}{e^{(z0\sqrt{\frac{\varepsilon_r+1.41}{87}})}} - 1.25 \times t \quad (11)$$

Where W_f is the width of the feed line?
z_0 be the impedance value, t be the trace thickness. Based on the known equation, the subsequent values are calculated.

Table 1. MIMO Patch antenna parameters

Circular & Hexagonal MIMO Patch Antenna Parameters	Dimensions
Width of the substrate	16mm
Length of the Substrate	20mm
Height of the Substrate	12mm
Constant of dielectric	2.2
Length of the Patch	1.895 mm
Input Impedance	50ohms
Width of the patch	3.950 mm

3.1.1 MIMO Antenna Performance and Proposed Meta-Material

The proposed MIMO-based antenna array based on the structure of metamaterial and its development is shown in Fig.1. The substrate which is FR-4 with relative permittivity of 3.9, 0.02 loss in tangent, and 1.7mm thickness designs are the main objectives of this work. MIMO antenna is 20x 16x12 mm3 in total. Four patch antennas with 50-Ohm coaxial feeding and a 2mm edge-to-edge antenna element distance comprise the MIMO antenna array. For minimization of mutual coupling, the metamaterial is integrated with the MIMO antenna and originates to be composed of four identical antennae which are based on the patch design edged by coaxial lines, with two metamaterial cells implanted in the FR-4 substrate to increase the MIMO antenna which is isolated. As a result, the slots are cut into the metamaterial's surface and their performance is assessed. Increasing the size of the antenna will significantly boost the gain. Hence, the suggested MIMO antenna and meta-material are optimized with help of HFSS and its parameter metrics. The MIMO antenna is analyzed and depicted in Fig.2 to acquire a better thought of the consequences of the suggested meta-material cells. Currents flow from one antenna patch to the next. Whenever presented 3-D metamaterial structure is integrated, the antenna induces very small surface currents. As a result, of a significant current flow on the 3-D structure of Metamaterial, the surface current is limited and

reduces the mutual coupling of the closed MIMO antenna.

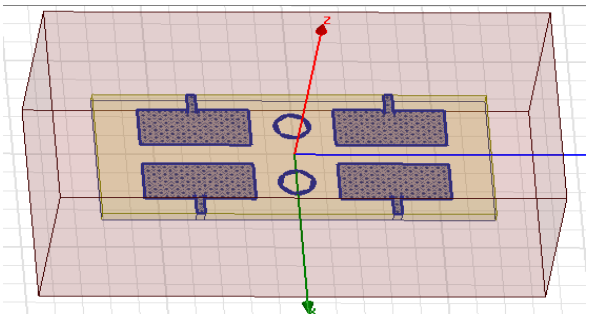

Fig. 2: Circular and hexagonal slot antennas are printed on an FR4 substrate.

Where, the impacts of the key parameters, impedance bandwidth, and MIMO antenna isolation on S11 and S21 are next demonstrated. The MIMO antenna's operating band is found to be max constant and isolated in terms of S12 being increased. The resonance frequency of a metamaterial is used to compute the split-ring resonator.

$$k = \frac{1}{2\pi\sqrt{LC}} \tag{12}$$

Scattering parameters are used to examine the antenna structure metamaterial property (S-Parameter). The reflectance (S11) and transmittance (S21) characteristics are used to compute the refractive index (n) and impedance (z), as shown in the equation below.

$$p = \frac{1}{jd} cos^{-1}[\frac{1}{2S_{21}}(1 - S_{11}^2 S_{21}^2)] \tag{13}$$

$$z = \sqrt{\frac{\left((1+S_{11}^2)-S_{21}^2\right)}{(1-S_{11}^2)-S_{21}^2)}} \tag{14}$$

$$\varepsilon = \frac{q}{z} \tag{15}$$

$$\mu = \frac{q}{z} \tag{16}$$

where q denotes the refractive index, d the substrate height, and j the is wave vector. The substrate wave impedance is z, the permittivity isε, and the permeability isμ. The antenna's resonance frequency, return loss, radiation pattern, and VSWR are all modeled. Copper, with a thickness of 1.6 mm, is used for the metamaterial elements, ground layer, and patch.

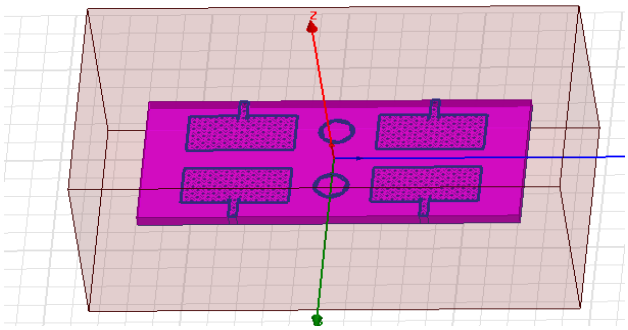

Fig. 3: Depicts a side view of the proposed antenna structure.

Fig.3 illustrates the proposed antenna from the side. Consequently, the projected antenna is powered via coaxial feed. ROGERS RT Duroid 5880 creates 1.6 mm thick substrates and metamaterial are positioned at the top of each superstrate. The circle metamaterial element has a diameter of 2 mm.

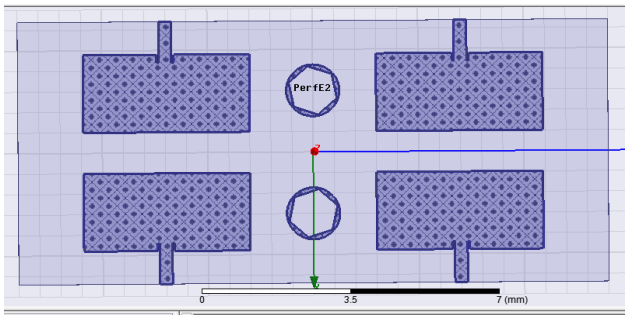

Fig. 4: Microstrip patch with the suggested antenna structure

Using varactor diode switching, a microstrip patch antenna with a circle and hexagonal array metamaterial superstrate is developed. A superstrate microstrip patch antenna, on the additional hand, increases gain and bandwidth as shown in Fig.4.

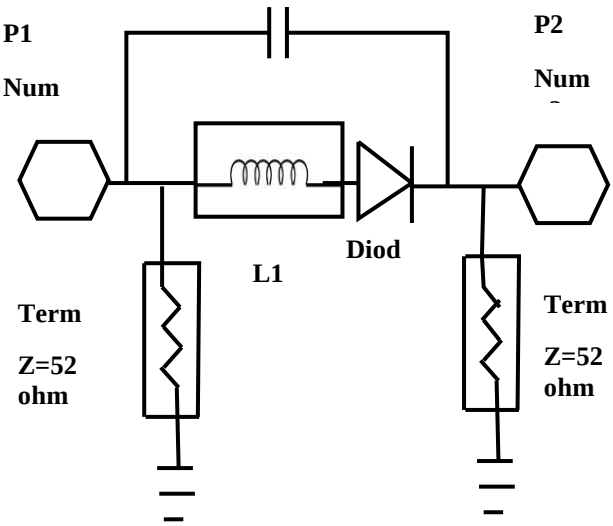

Fig. 5: Varactor diode equivalent circuit
The frequency ranges can be reconfigured with the use of a reconfigurable antenna. Consequently, the varactor diode is used in the reconfigurable antenna to accelerate the speed of frequency tuning. This diode is critical in a reconfigurable antenna. Where variable capacitor formation is based on its varying capacitance value, the reverse bias voltage changes, and so does the antenna's frequency at which it is operating, junction capacitance, and current distribution. Figure 5 depicts the varactor diode equivalent circuit. Tuning the varactor diode in the proposed antenna design affects the capacitance of the diode, which changes the antenna current distribution. Also, it is re-configured for various frequencies. The varactor capacitance can only be accustomed within a definite range. To optimize antenna properties such as frequency, bandwidth, and beam width, a novel foraging, and navigation optimization algorithm has been given. Hence, the antenna parameters are optimized by altering the metamaterial superstrate permeability and permittivity values.

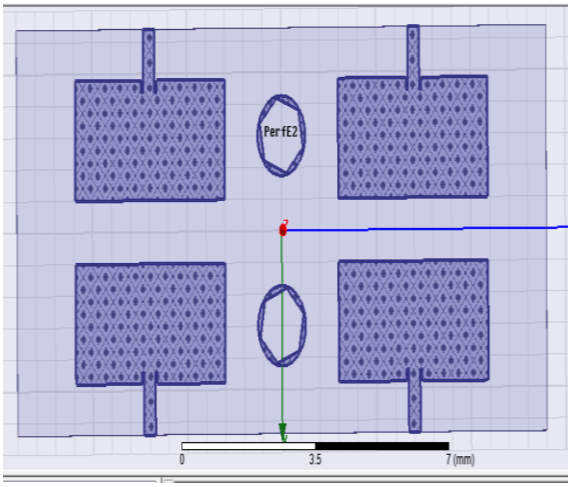

Fig. 6: 3D view of circle and Hexagonal shaped metamaterial with superstrate antenna(Complete Antenna structure)

Fig.6 depicts a suggested superstrate antenna system with a three-dimensional array of circular and hexagonal-shaped metamaterial elements. The results are also contrasted with a previously published design. Our proposed architecture, which employs a metamaterial superstrate, achieves the highest gain with the least mutual coupling.

4 Results and Discussion

This section includes a comprehensive description of the implementation findings, as well as the performance of our proposed framework, as well as a comparative analysis to guarantee that our suggested framework outperforms the existing approaches in the metamaterial superstrate.

4.1 Specification of Software

The proposed design is fabricated using HFSS which is Ansys software and is a recent technology and widely used for electromagnetic structures solver. It's one of several industry tools for antenna design and RF electronic circuits are more sophisticated and developed recently for MIMO antenna designed for filtering, packaging, and also for transmission lines.

4.2 Simulation Results and Performance Evaluation

The Circular and Hexagonal MIMO patch array for 5G Technology with reduced Mutual Coupling using Metamaterial Superstrate results are discussed in this section. Each design is illustrated individually, and the output is provided.

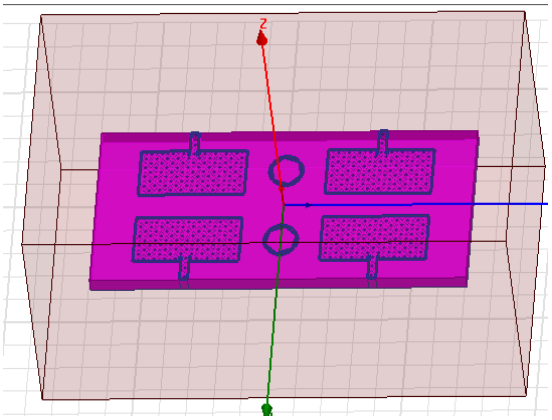

Fig. 7: HFSS software is utilized to design.

Fig.7 displays the design of a microstrip patch antenna, and the length and width of the antenna are determined based on the frequency employed, in this instance millimeter-wave frequency.

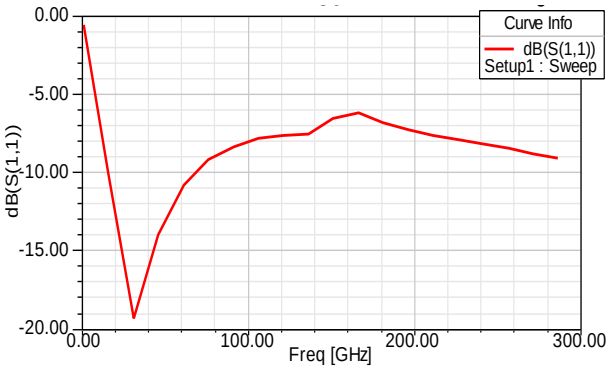

Fig. 8: A return loss of -19.2dB is measured at a resonance frequency of 29GHz.

At a resonant frequency of 29 GHz of -19.2dB return loss is produced. This shift occurs as a result of the metamaterial layer property, which allows us to reduce the antenna size are shown in Fig 8. It is also a measure of the mismatch between the load and the transmission line. As the impedance mismatch rises. VSWR in a standing wave is formulated between the ratio of the maximum voltage and the minimum voltage. Hence, $VSWR = \frac{V_{max}}{V_{min}}$ is a formula for calculating the VSWR.

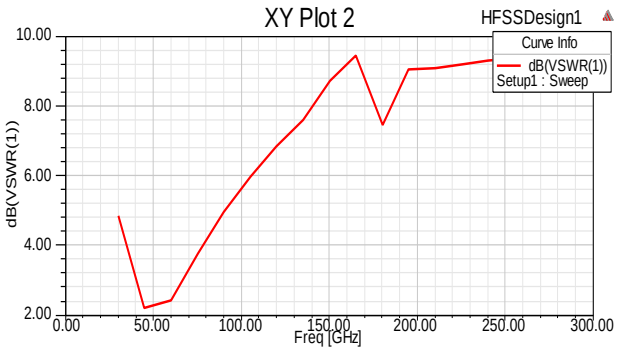

Fig. 9: VSWR Vs Frequency

As shown in the graph Fig.9, the VSWR value is 1.9dB. This could have a significant impact on antenna gain. The return loss is investigated using scattering (S) parameters. Return loss is the signal power loss due to impedance mismatching. A high VSWR denotes a higher return loss. The return loss plot or VSWR can also be used to calculate bandwidth.

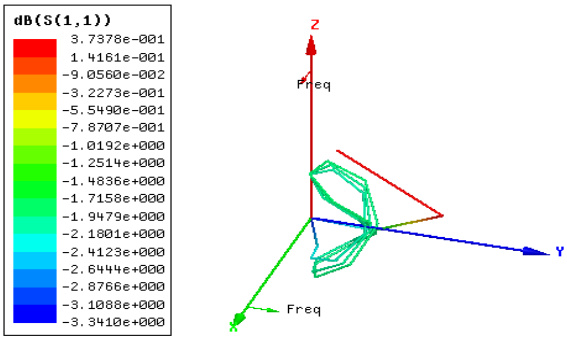

Fig. 10: Gain for circle and Hexagonal shaped metamaterial with superstrate antenna

Gain is among the realized quantities in antenna theory. Where the advantage is lower than in the typical case of directivity. There are ohmic and other losses presented. The act of transforming input power into radio waves in a certain direction is known as gain. The simulated maximum gain of a full antenna is 3.73 dB, as illustrated in Fig10.

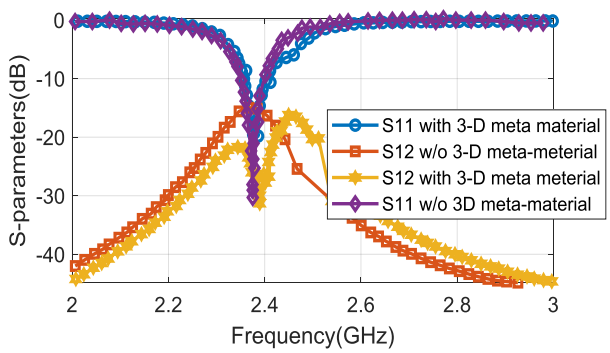

Fig. 11: MIMO antenna impedance bandwidth and mutual coupling

The 3-D metamaterial cells anticipated are then integrated into the manufactured element MIMO antenna array. The HFSS is used to compare the simulation results of the MIMO antenna with and without the recommended meta-material in Fig. 11. The proposed MIMO antenna has a bandwidth of around 33.4MHz, as can be shown and the MIMO resonance frequency is almost the same. However, as compared to a MIMO antenna without the proposed 3-D metamaterial cells, the antenna with proposed meta-material cells has a -18 dB with mutual coupling. That is, the projected MIMO antenna with 3D metamaterial cells considerably enhances isolation while reducing mutual coupling.

4.3 Comparison Analysis

This section describes the simulation outputs of the proposed framework as well as the comparative analysis.

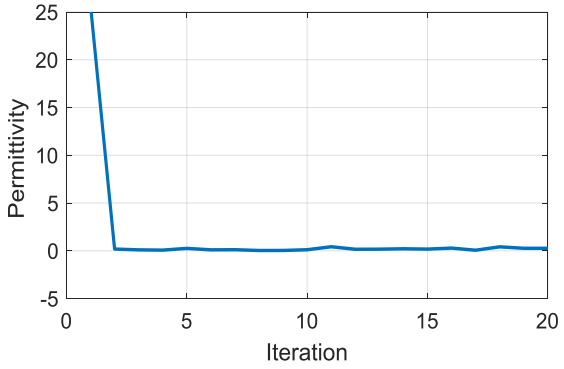

Fig. 12: Different iteration Vs Permittivity

Permittivity is a measure of how easily charges align in the presence of an electric field (polarize). Higher permittivity implies greater resistance to the production of an electric field and slower disturbance propagation in the medium. Fig.12 shows how the permittivity falls as the iteration number increases.

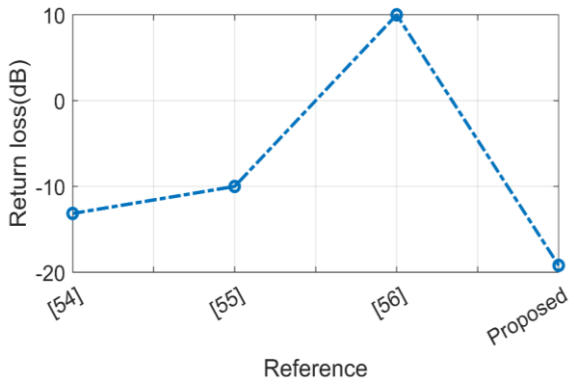

Fig. 13: Return loss(dB)

Fig.13. and Table 2 depict the comparative study of the return loss with the existing techniques [54-56]. The return loss of the suggested technique achieves -19.2 dB, which is -9.2dB higher than the [55] and -6 dB higher than the [54].

Table 2. Comparison of Return loss (dB)

Ref.	Technique used	Return loss
[54]	Metamaterial Superstrate Antenna with Modified Slot Size in Uniform Structure.	-13.15dB
[55]	Wideband antenna design	-10dB
[56]	MIMO antenna	10dB
Proposed	**MIMO patch antenna array using metamaterial superstrate.**	**-19.2dB**

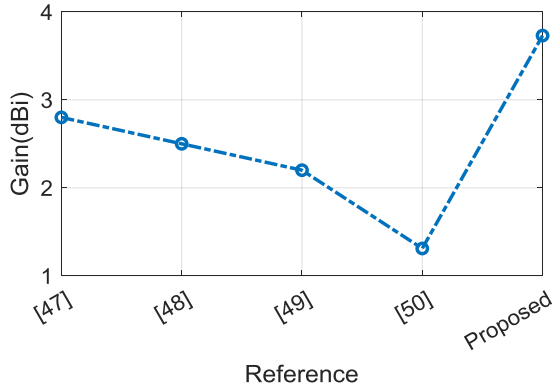

Fig. 14: Gain(dB) Vs Proposed Gain

Fig.14 and Table 3 provide a comparison of the gain (dB) with known approaches [47-50]. The proposed technique produces a gain of 3.73dBi, which is 2.4dB higher than the [50].

Table 3. Comparison of Gain(dB)

Ref.	Technique used	Gain
[47]	Double element square ring slot	2.5–2.8 dBi
[48]	An inductor with a staircase-shaped linked ground strip	1.4–2.5 dBi
[49]	T-shaped feed, inverted E and U shaped stubs	2.2 dBi
[50]	Meandered meta-material	1.31 dBi
	MIMO patch antenna array using metamaterial superstrate	**3.73dBi**

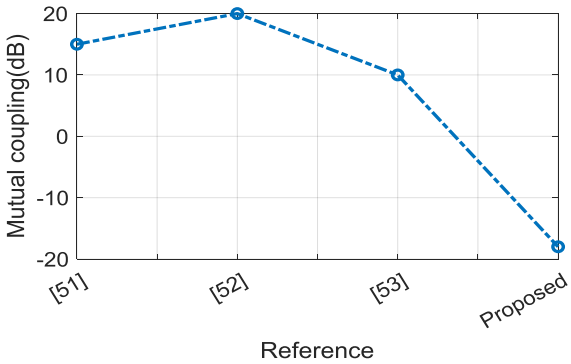

Fig. 15: Mutual coupling (dB)

Fig.15 and Table 4 show a comparison of mutual coupling (dB) with existing techniques [51-53]. Where the proposed technique achieves reduced mutual coupling of -18 dB using metamaterial superstrate.

Table 4. Comparison of mutual coupling (dB)

Ref.	MIMO antenna details	Mutual coupling
[51]	Radiating element: staircase-shaped Substrate: FR4	15 dB
[52]	Radiating element: E-shaped tree structure Substrate: FR4	Above 20 dB
[53]	Radiating element: two spider-shaped radiating patches Substrate: FR4	$\leq$ 10dB
Proposed	**Radiating element: Honey comb-shaped using metamaterial superstrate.**	**-18dB**

5 Conclusion

Analyses of MIMO patch antennas with circular and hexagonal arrays of metamaterial superstrate are supported using varactor diode switching. By employing a superstrate microstrip patch antenna, gain and return loss are improved. With a bandwidth of 33.4MHz, the proposed metamaterial superstrate architecture achieves a maximum gain of 3.73dBi. Thus, the suggested antenna demonstrated that it meets the requirements of having a wider bandwidth, being compact, having a stable radiation pattern, and having a relatively higher gain. Hence, the MIMO patch antenna array for 5G technology with a minimum mutual coupling of -18dB was developed efficiently using the proposed metamaterial superstrate, predominantly in mm-wave applications. The experimental results show that the proposed framework outperforms the others in terms of resonant frequency at 29GHz and return loss of -19.2dB. The antenna structure with 29GHz and return loss of -19.2dB can be manipulated and reconfigured with different properties as a lumped parameter using a resistor for high frequency.

References:

[1]. Arati Manjeshwar, et.al, "APTEEN: A Hybrid Protocol for Efficient Routing and Comprehensive Information Retrieval in Wireless Sensor Networks", 1530-2075/02, IEEE, 2002

[2]. Andrews, J.G.; Buzzi, S.; Choi, W.; Hanly, S.V.; Lozano, A.; Soong, A.C.; Zhang, J.C. What will 5G be? IEEE J.Sel. Areas Commun. 2014, 32, 1065–1082.

[3]. Y. Niu, Y. Li, D. Jin, L. Su, and A. V. Vasilakos, "A survey of millimeter-wave communications (mm-wave) for 5g: opportunities and challenges," Wireless Networks, vol. 21, no. 8, pp. 2657–2676, 2015.

[4]. A. Morgado, K. M. S. Huq, S. Mumtaz, and J. Rodriguez, "A survey of 5g technologies: regulatory, standardization and industrial perspectives," Digital Communications and Networks, vol. 4, no. 2, pp. 87–97, 2018.

[5]. X. Ge, S. Tu, G. Mao, C.-X. Wang, and T. Han, "5g ultra-dense cellular networks," IEEE Wireless Communications, vol. 23, no. 1, pp. 72–79, 2016.

[6]. M. M. Lodro and S. Greedy, "A short review on progress for 5g mm-wave cellular communication networks." 2016.

[7]. J. Zhang, M. Shafi, A. F. Molisch, F. Tufvesson, S. Wu, and K. Kitao, "Channel models and measurements for 5g," IEEE Communications Magazine, vol. 56, no. 12, pp. 12–13, 2018.

[8]. M. M. Lodro, N. Majeed, A. A. Khuwaja, A. H. Sodhro, and S. Greedy, "Statistical channel modeling of 5g mm-wave MIMO wireless communication," in Computing, Mathematics and Engineering Technologies (iCoMET), 2018 International Conference on. IEEE, 2018, pp. 1–5

[9]. Misilmani H M E and El-Hajj A M 2017 Massive MIMO Design for 5G Networks: An Overview on Alternative Antenna Configurations and Channel Model Challenges. In: 2017 International Conference on High Performance Computing & Simulation (HPCS), pp 288-94.

[10]. Tong W and Peiying Z 2016 Huawei - 5G: A Technology Vision Huawei Technical Publications.

[11]. M. A. Jensen and J. W. Wallace, "A review of antennas and propagation for MIMO wireless communications," IEEE Transactions on Antennas and Propagation, vol. 52, no. 11, pp. 2810– 2824, 2004.

[12]. J. Park and B. Clerckx, "Multi-User linear precoding for multi polarized massive MIMO system under imperfect CSIT," IEEE Transactions on Wireless Communications, vol. 14, no. 5, pp. 2532–2547, 2015.

[13]. Zhang, L., T. Jiang, and Y. Li, "Design of a high isolation dual-band MIMO antenna for WLAN and WIMAX applications," PIERS Proceedings, 1593–1597, Prague, July 6–9, 2015.

[14]. Zulkifli, F. Y., and E. T. Rahardjo, "Compact MIMO microstrip antenna with the defected ground for mutual coupling suppression," PIERS Proceedings, 89–92, Marrakesh, Morocco, March 20–23, 2011.

[15]. Bansod, B. H., "Compact two-port MIMO microstrip antenna for 4G applications," Interna-2682 2017 Progress In Electromagnetics Research Symposium — Fall (PIERS — FALL), Singapore, 19–22 November national Conference on Information Processing Vishwakarma Institute of Technology, 571–574, Pune, India, December 2015.

[16]. Sharawi, M.-S.: 'Printed multi-band MIMO antenna systems and their performance metrics', IEEE Antennas Propag. Mag., 2013, **55**, (5), pp. 218– 232.

[17]. Roy, S.; Chakraborty, U. Mutual Coupling Reduction in a Multi-band MIMO Antenna Using Meta-Inspired Decoupling Network Wirel. Pers. Commun. **2020**, 114, 3231–3246.
[18]. Nadeem, I.; Choi, D. Study on Mutual Coupling Reduction Technique for MIMO Antennas. IEEE Access **2019**, 7, 563–586.
[19]. Chen, X.; Zhang, S.; Li, Q. Review of mutual coupling in MIMO systems. IEEE Access 2018, 6, 24706–24719.
[20]. Chouhan1, S.; Panda2, D.K.; Gupta, M.; Singhal, S. Multiport MIMO antennas with mutual coupling reduction techniques for modern wireless transceiver operations: A review. Int. J. RF Microw. Comput. Aided Eng. **2017**, 28, 1–13.
[21]. C.-M. Luo, J.-S. Hong, and L.-L. Zhong, ``Isolation enhancement of a very compact UWB-MIMO slot antenna with two defected ground structures," IEEE AntennasWireless Propag. Lett., vol. 14, pp. 1766_1769,Apr. 2015.
[22]. B. K. Lau and J. B. Andersen, ``Simple and ef_cient decoupling of compact arrays with parasitic scatterers," IEEE Trans. Antennas Propag., vol. 60, no. 2, pp. 464_472, Feb. 2012.
[23]. H. Yi and S. Qu, ``A novel dual-band circularly polarized antenna based on electromagnetic band-gap structure," IEEE Antennas Wireless Propag.Lett., vol. 12, pp. 1149_1152, Sep. 2013
[24]. Q. Li, A. P. Feresidis, M. Mavridou, and P. S. Hall, ``Miniaturized double-layer EBG structures for broadband mutual coupling reduction between UWB monopoles," IEEE Trans. Antennas Propag., vol. 63, no. 3, pp. 1168_1171, Mar. 2015.
[25]. A. Pirhadi1, H. Bahrami, and A. Mallahzadeh, ``Electromagnetic bandgap (EBG) superstrate resonator antenna design for monopulse radiation pattern," Appl. Comput. Electromagn. Soc. J., vol. 27, no. 11, pp. 908_917, 2012.
[26]. S. Wang and Z. Du, ``Decoupled dual-antenna system using crossed neutralization lines for LTE/WWAN smartphone applications," IEEE Antennas Wireless Propag. Lett., vol. 14, pp. 523_526, Nov. 2015.
[27]. H. Qi, L. Liu, X. Yin, H. Zhao, and W. J. Kulesza, ``Mutual coupling suppression between two closely spaced microstrip antennas with an asymmetrical coplanar strip wall," IEEE Antennas Wireless Propag. Lett., vol. 15, pp. 191_194, Jun. 2016.
[28]. S.-H. Zhu, X.-S. Yang, J. Wang, N.-S. Nie, and B.-Z. Wang, ``Mutual coupling reduction of _45_ dual-polarized closely spaced MIMO antenna by topology optimization," IEEE Access, vol. 8, pp. 29089_29098, 2020.
[29]. K.-L. Wu, C. Wei, X. Mei, and Z.-Y. Zhang, ``Array-antenna decoupling surface," IEEE Trans. Antennas Propag., vol. 65, no. 12, pp. 6728_6738, Dec. 2017.
[30]. S. Zhang, X. Chen, and G. F. Pedersen, ``Mutual coupling suppression with decoupling ground for massive MIMO antenna arrays," IEEE Trans. Veh. Technol., vol. 68, no. 8, pp. 7273_7282, Aug. 2019.
[31]. M. Li, B. G. Zhong, and S. W. Cheung, ``Isolation enhancement for MIMO patch antennas using near-_eld resonators as coupling-mode transducers," IEEE Trans. Antennas Propag., vol. 67, no. 2, pp. 755_764, Feb. 2019.
[32]. C. F. Ding, X. Y. Zhang, C.-D. Xue, and C.-Y.-D. Sim, ``Novel pattern diversity-based decoupling method and its application to multi-element MIMO antenna," IEEE Trans. Antennas Propag., vol. 66, no. 10, pp. 4976_4985, Oct. 2018.
[33]. H. Li, B. K. Lau, Z. Ying, and S. He, ``Decoupling of multiple antennas in terminals with chassis excitation using polarization diversity, angle diversity and current control," IEEE Trans. Antennas Propag., vol. 60, no. 12, pp. 5947_5957, Dec. 2012.
[34]. J. Ghosh, D. Mitra, and S. Das, ``Mutual coupling reduction of slot antenna array by controlling surface wave propagation," IEEE Trans. Antennas Propag., vol. 67, no. 2, pp. 1352_1357, Feb. 2019
[35]. J.-Y. Lee, S.-H. Kim, and J.-H. Jang, ``Reduction of mutual coupling in planar multiple antennae by using 1-D EBG and SRR structures," IEEE Trans. Antennas Propag., vol. 63, no. 9, pp. 4194_4198, Sep. 2015.
[36]. Z. Wang, L. Zhao, Y. Cai, S. Zheng, and Y. Yin, ``A meta-surface antenna array decoupling (MAAD) method for mutual coupling reduction in a MIMO antenna system," Sci. Rep., vol. 8, no. 1, Feb. 2018, Art. no. 3152
[37]. L. Si, H. Jiang, X. Lv, and J. Ding, ``Broadband extremely close-spaced 5G MIMO antenna with mutual coupling reduction using metamaterial inspired superstrate," Opt. Express, vol. 27, no. 3, pp. 3472_3482, 2019.

[38]. F. Liu, J. Guo, L. Zhao, X. Shen, and Y. Yin, ``A meta-surface decoupling method for two linear polarized antenna arrays in sub-6 GHz base station applications," IEEE Access, vol. 7, pp. 2759_2768, 2019.

[39]. A. Jafargholi, A. Jafargholi, and J. H. Choi, ``Mutual coupling reduction in an array of patch antennas using CLL metamaterial superstrate for MIMO applications," IEEE Trans. Antennas Propag., vol. 67, no. 1, pp. 179_189, Jan. 2019.

[40]. F. Liu, J. Guo, L. Zhao, G.-L. Huang, Y. Li, and Y. Yin, ``Dual-band metasurface-based decoupling method for two closely packed dual-band antennas," IEEE Trans. Antennas Propag., vol. 68, no. 1, pp. 552_557, Jan. 2020

[41]. X.-J. Zou, G.-M. Wang, Y.-W. Wang, and H.-P. Li, ``An efficient decoupling network between feeding points for multielement linear arrays," IEEE Trans. Antennas Propag., vol. 67, no. 5, pp. 3101_3108, May 2019.

[42]. T. S. Rappaport, J. N. Murdock, and F. Gutierrez, "State of the art in 60-GHz integrated circuits and systems for wireless communications," Proceedings of the IEEE, vol. 99, no. 8, pp. 1390-1436, Aug. 2011.

[43]. IEEE802.15.3c-2009, Part 15.3: Wireless Medium Access Control (MAC) and Physical Layer (PHY) Specifications for High Rate Wireless Personal Area Networks (WPANs), Amendment 2: Millimeter-wave-based Alternative Physical Layer Extension, Oct. 2009.

[44]. Thummaluru, S.-R., Chaudhary, R.-K., 'Mu negative meta-material filter based isolation technique for MIMO antennas', Electron. Lett., 2017, **53**, (10), pp. 644–646.

[45]. Jafargholi, A., Jafargholi, A., Choi, J.-H.: 'Mutual coupling reduction in an array of patch antennas using CLL metamaterial superstrate for MIMO applications, IEEE Trans. Antennas Propag., 2019, **67**, (1), pp. 179–189.

[46]. L. Si, H. Jiang, X. Lv, and J. Ding, ``Broadband extremely close-spaced 5G MIMO antenna with mutual coupling reduction using metamaterial inspired superstrate," Opt. Express, vol. 27, no. 3, pp. 3472_3482, 2019.

[47]. Ojaroudi Parchin, Naser, et al. "Multi-band MIMO antenna design with a user-impact investigation for 4G and 5G mobile terminals." Sensors 19.3 (2019): 456.

[48]. Yang, Ming, Yufa Sun, and Fan Li. "A compact wideband printed antenna for 4G/5G/WLAN wireless applications." International Journal of Antennas and Propagation 2019 (2019)

[49]. Desai, Arpan, et al. "Multiband inverted E, and U-shaped compact antenna for Digital broadcasting, wireless, and sub 6 GHz 5G applications." AEU-International Journal of Electronics and Communications 123 (2020): 153296.

[50]. Patel, Shobhit K., and Y. P. Kosta. "Meandered multiband metamaterial square microstrip patch antenna design." Waves in Random and Complex Media 22.4 (2012): 475-487.

[51]. Chouhan, Sanjay, et al. "Spider-shaped fractal MIMO antenna for WLAN/WiMAX/Wi-Fi/Bluetooth/C-band applications." AEU-International Journal of Electronics and Communications 110 (2019): 152871

[52]. Addepalli, Tathababu, and Vaddinuri Rajareddy Anitha. "Design and parametric analysis of hexagonal-shaped MIMO patch antenna for S-band, WLAN, UWB, and X-band applications." Progress In Electromagnetics Research C 97 (2019): 227-240

[53]. Gao, Peng, et al. "Compact printed UWB diversity slot antenna with 5.5-GHz band-notched characteristics." IEEE Antennas and Wireless Propagation Letters 13 (2014): 376-379

[54]. Kavitha, K., and K. Seyatha. "Metamaterial superstrate antenna design with gain enhancement." International Journal of Applied Engineering Research 13.24 (2018): 16939-16944.

[55]. Nazli, Nur Farzana Mohd, and Imran Mohd Ibrahim. "Wideband antenna design for sub 6GHz range for 5G application." INOTEK 2021 1 (2021): 25-26.

[56]. Lee, Youngkin, et al. "Design of a MIMO antenna with improved isolation using meta-material." 2011 International Workshop on Antenna Technology (iWAT). IEEE, 2011.

Contribution of Individual Authors to the Creation of a Scientific Article (Ghostwriting Policy)

The authors equally contributed in the present research, at all stages from the formulation of the problem to the final findings and solution.

Sources of Funding for Research Presented in a Scientific Article or Scientific Article Itself

No funding was received for conducting this study.

Conflict of Interest

The authors have no conflicts of interest to declare that are relevant to the content of this article.